Electromagnetic Analysis of a Novel Switched-Flux Memory Machine Employing a Parallelogram Hysteresis Model

Hui Yang, Heyun Lin*, *Member, IEEE*, Jianning Dong, Jianhu Yan, Yunkai Huang and Shuhua Fang
Engineering Research Center for Motion Control of Ministry of Education, Southeast University, Nanjing 210096, China
* hyling@seu.edu.cn

***Abstract*—A novel surface-mounted permanent magnet switched-flux memory machine (SPMSFMM) is proposed by incorporating the flux-mnemonic mechanism of aluminum-nickel-cobalt (AlNiCo) PM into the switched-flux PM machine (SFPMM). It employs surface-mounted PMs radially magnetized to enhance the PM utilization rate. The constructional characteristics and operational principle of the SPMSFMM are described and stated respectively. Additionally, a time-divisional pulsed-current applying strategy is developed to equalize the PM magnetization status. The proposed machine exhibits relatively high power density, sinusoidal back-electromotive force (EMF) waveform and sound fault-tolerant capability. Furthermore, the time-stepping finite element method (TSFEM) integrated with a multi-layer parallelogram hysteresis model (MPHM), accounting for the localized hysteresis loops of AlNiCo, is performed to evaluate the electromagnetic performance precisely. The TSFEM predictions are quantitatively compared with the nonlinear equivalent magnetic circuit model (NEMCM), where good agreement between two predicted techniques is achieved.**

***Index Terms*—Electromagnetic analysis, hysteresis model, memory machine, permanent magnet, switched-flux**

I. Introduction

Recently, an embranchment of genuinely variable flux permanent magnet (PM) machine, memory machine, which employs aluminum-nickel-cobalt (AlNiCo) PM with innate low coercivity and high remanence, is of growing concerns due to its remarkable flux-tunable capability achievable by varying the magnetization level of PM at the cost of neglectable additional excitation loss, hence exhibiting significant feasibility for electric vehicle (EV) application [1].

This paper proposes a novel surface-mounted PM switched-flux memory machine (SPMSFMM) by integrating the flux-mnemonic concept with the switched-flux machine, to achieve eminent electromagnetic performance integrated with wide-range flux controllability [2-4]. The configuration of the proposed SPMSFMM is depicted in Fig. 1, which adopts a three-phase 12/7-pole topology. The field teeth for the surface-mounted PMs and the armature teeth for enwinding the armature windings distribute in the stator alternately. In addition, the radially magnetized AlNiCo PMs are accommodated at the tips of the field stator teeth with opposite polarity successively; whilst the twin 3-phase concentrated windings contribute as the armature windings. The cylindrical rotor is composed of 7-segment laminated cores with sector shape, a non-magnetic sleeve and shaft.

Since the hysteresis nonlinearity of AlNiCo PM inevitably complicates the numerical process, a multi-layer parallelogram hysteresis model (MPHM) is proposed to investigate the repetitive remagnetization or demagnetization physics of the AlNiCo PMs. The time-stepping finite element method (TSFEM) coupled with the MPHM is adopted to analyze the electromagnetic performance of the proposed machine. Further, the nonlinear equivalent magnetic circuit model (NEMCM) of SPMSFMM is constructed for rapid performance prediction [5], and the comparison of the predictions derived by the two aforementioned computational techniques is quantitatively provided.

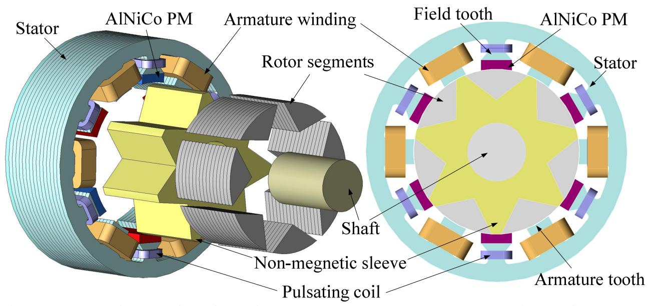

Fig. 1. Topology of 12/7-pole SPMSFMM. (a) Cutaway view. (b) Cross-sectional view.

II. Implementation of TSFEM Coupled with MPHM

The MPHM of AlNiCo PM is proposed as depicted in Fig. 2, where, for simplification, it is supposed that the major loop and all minor loops are linearized to parallelogram shapes, which consist of a series of parallel edges with different values of coercivity and remanence B_{rk}. The set of branch lines labeled with l_1 and l_2 can be respectively expressed as:

$$B = \mu_0 \mu_r H_m + B_{rk}, n = 1, 2, 3... . \quad (1)$$

$$B = \frac{\mu_0 \mu_r H_m + B_{r1}}{H_m - pH_c}\left(H + pH_c\right) \quad (2)$$

where μ_0 is the vacuum permeability, μ_r is the relative permeability of AlNiCo magnet, H_m is the positive magnetic field intensity, B_{rk} represents the corresponding k^{th} remanence of sets of the hysteresis loops, and p is defined as the adjusting coefficient, belonging to [-1, 1].

By integrating (1) and (2), the H value of point M at the first quadrant and knee point N at the second quadrant, which donate the criterion of adjustment of PM operating point, can be deduced as:

$$H_{nk(mk)} = \frac{H_m B_{rk} - (\mu_0 \mu_r H_m + B_{r1} + B_{rk}) p H_c}{\mu_0 \mu_r p H_c + B_{r1}} \quad (3)$$

The FEM is applied to calculate the initial flux intensity H_0 by setting all PM elements zero B_r and constant μ_r, and the auxiliary function for initializing the MPHM is governed by

$$B_0 = \mu_0 \left(H + \frac{a_1 H_0 + a_2 H_0 |H_0|}{1 + b_1 |H_0| + b_2 H_0^2} \right) \quad (4)$$

where the coefficient can be obtained by experimentally fitting.

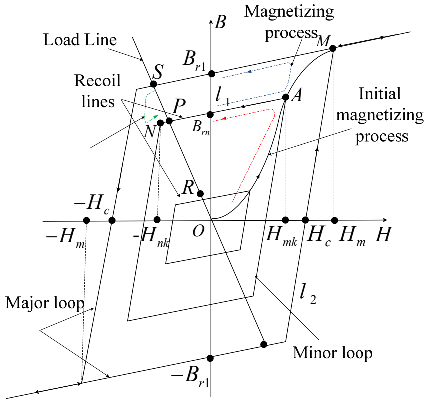

Fig. 2. MPHM of AlNiCo PM.

During the magnetization initialization, the corresponding working recoil lines of PM element will be determined by TSFEM combined with (4), while the PM operating point will be specified according to the quantitative comparison between the applying magnetizing/demagnetizing flux intensity and the saturated H value, i.e. H_{mk} or H_{nk}, during the flux adjustment.

III. Establishment of NEMCM

Fig. 3 shows a simplified NEMCM for the SPMSFMM, in which Λ_S donates the equivalent slot permenance, the PM and the stator winding can be modeled as a flux source Φ_M with permenance Λ_M and MMF source F_w respectively. Since the air-gap permenance varies with the rotation of rotor, the permenances of the divided air regions are adaptively given as:

$$\Lambda_{a1} = \frac{\mu_0 S_i}{g} = \frac{\mu_0 (R_{si} + R_{ro})}{2g} \frac{\pi}{180} l_a \quad (5)$$

$$\Lambda_{a2,3} = \frac{2\mu_0 L_a}{\pi} ln \left(1 + \frac{\pi X_1}{\pi R_1 + 2g} \right) \quad (6)$$

where S_i, g, R_{si} and R_{ro} are the cross-sectional area, the length of air-gap, the inner radius of the stator and the outer radius of the rotor respectively. Hence, the total air-gap permeance regarding the two adjacent stator pole faces can be deduced by summing Λ_{a1}~Λ_{a3}.

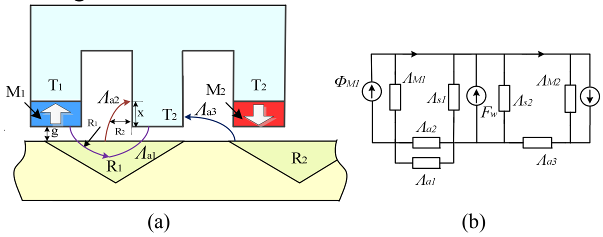

Fig. 3. NEMCM of a section of SPMSFMM. (a) Typical machine section. (b) NEMCM.

IV. Electromagnetic Performance Investigation

Both the TSFEM coupled with MPHM and the NEMCM are performed to investigate the electromagnetic performance of the proposed SPMSFMM

It can be seen in Fig. 4 that the no-load magnetic field distribution varies markedly by temporarily applying the pulsed currents with peak values of +8A, +6A, -3A and -5A, respectively. It should be noted that the intermediate parts of PMs are more magnetically susceptible to the pulsed MMF than the two-sided counterparts.

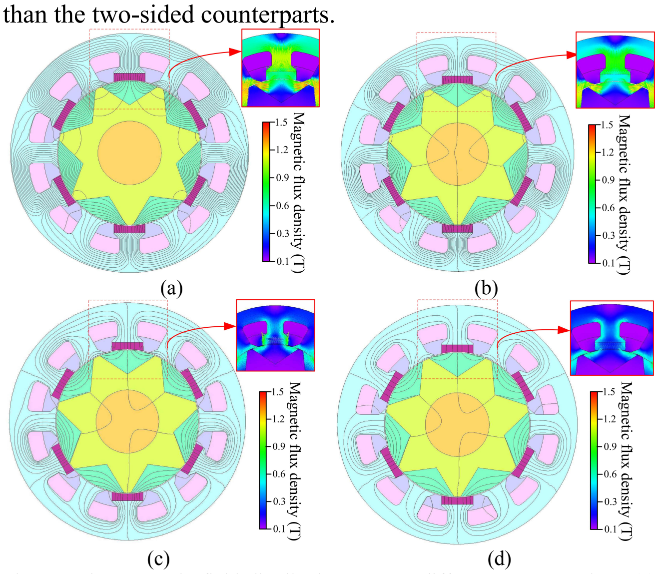

Fig. 4. The magnetic field distributions versus different current pulses. (a) +8A. (b) +6A. (c) -3A. (d) -5A.

V. Conclusions

In this paper, a novel SPMSFMM has been proposed and its topology is described. The static electromagnetic performance of the SPMSFMM is evaluated by the TSFEM dynamically coupled with the MPHM and the NEMCM respectively. Satisfactory agreement between the foregoing predictions identifies the correctness of MPHM and validity of the proposed SPMSFMM with reference to the remarkable online flux controllability and the sinusoidal flux linkage and the back-EMF, which is desirable for brushless AC operation.

The detailed analysis results regarding the electromagnetic performance evaluation will be presented in the full paper.

References

[1] V. Ostovic, “Memory motors: A new class of controllable-flux permanent magnet machines for true wide-speed operation,” *IEEE Ind. Appl. Mag.*, vol. 9, no. 1, pp. 52–61, Jan./Feb. 2003.

[2] Liu Hengchuan, Lin Heyun, Fang Shuhua, and Z. Q. Zhu, "Permanent magnet demagnetization physics of a variable flux memory motor," *IEEE Trans. on Magn.*, vol. 45, no.10, pp. 4736-4739, Oct. 2009.

[3] Liu Hengchuan, Lin Heyun, Z. Q. Zhu, Huang Mingming, and Jin Ping, "Permanent magnet remagnetizing physics of a variable flux memory motor," *IEEE Trans. on Magn.*, vol. 46, no.6, pp. 1679-1682, Jun. 2010.

[4] L. Wenlong, K. T. Chau, G. Yu, J. Z. Jiang, and L. Fuhua, "A new flux-mnemonic dual-magnet brushless machine," *IEEE Trans. on Magn.*, vol. 47, no.10, pp. 4223-4226, Oct. 2011.

[5] C. Yu, Z. Q. Zhu, and D. Howe, "Three-dimensional lumped-parameter magnetic circuit analysis of single-phase flux-switching permanent-magnet motor," *IEEE Trans. Ind. Appl.,* vol. 44, pp. 1701-1710, Nov./Dec. 2008.